

Collapse-Aware Triplet Decoupling for Adversarially Robust Image Retrieval

Qiwei Tian¹ Chenhao Lin¹ Zhengyu Zhao¹ Qian Li¹ Chao Shen¹

Abstract

Adversarial training has achieved substantial performance in defending image retrieval against adversarial examples. However, existing studies in deep metric learning (DML) still suffer from two major limitations: *weak adversary* and *model collapse*. In this paper, we address these two limitations by proposing collapse-aware triplet decoupling (CA-TRIDE). Specifically, TRIDE yields a strong adversary by spatially decoupling the perturbation targets into the anchor and the other candidates. Furthermore, CA prevents the consequential model collapse, based on a novel metric, collapseness, which is incorporated into the optimization of perturbation. We also identify two drawbacks of the existing robustness metric in image retrieval and propose a new metric for a more reasonable robustness evaluation. Extensive experiments on three datasets demonstrate that CA-TRIDE outperforms existing defense methods in both conventional and new metrics.

1. Introduction

Thanks to the massive image data and the development of Deep Neural Networks (DNNs), image retrieval has experienced substantial development. Despite their effectiveness, image retrieval systems are known to be vulnerable to adversarial examples, i.e. test samples that cause erroneous model behaviour [19]. Existing work on adversarial attacks against DNN-based image retrieval has explored deep metric learning (DML) models [9, 8, 2, 32] and deep hashing models [1, 10].

To defend DML models against adversarial examples, recent studies [33, 31] have modified the commonly-used adversarial training [11] from the domain of image classification

¹Xi'an Jiao Tong University, Xi'an, China. Correspondence to: Qiwei Tian <michaeltqw@stu.xjtu.edu.cn>, Chenhao Lin <linchenhao@xjtu.edu.cn>, Zhengyu Zhao <zhengyu.zhao@xjtu.edu.cn>, Qian Li <qianlix@xjtu.edu.cn>, Chao Shen <chaoshen@mail.xjtu.edu.cn>.

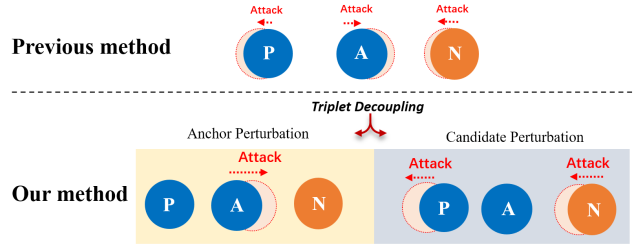


Figure 1. Our defense vs. the previous defense. Specifically, we address the *weak adversary* by decoupling the perturbation updates on anchors (A) and positive (P)/negative (N) candidates to maximize embedding shifts.

into the domain of image retrieval. However, these methods still suffer from two main limitations:

- **Weak adversary** is a widely overlooked issue since existing defenses [31, 33] directly adopt the perturbation strategy from the image classification domain without fully exploiting the triplet structure in image retrieval, which consists of three components: positive candidates, negative candidates, and anchors. As shown in Figure 1, the existing method perturbs all three components simultaneously and consequently distributes the desired perturbation among each component, represented by the small red shadows, leading to the smallest embedding shifts. Detailed qualitative analysis is given in the Appendix A .
- **Model Collapse** is a notorious challenge in DML, impeding researchers from training models with hard samples [27]. A collapsed model embeds all samples disastrously close and cannot appropriately retrieve semantically similar examples. Model collapse becomes inevitable in adversarial training as AT essentially aims at increasing sample hardness. The current state-of-the-art adversarial training method, hardness manipulation [31], avoids model collapse by restricting perturbation strength, consequently lowering its gained robustness.

In this paper, we aim to address the above two limitations by proposing a novel adversarial training approach to robust image retrieval, called **collapseness-aware triplet decoupling**

(CA-TRIDE). The core idea of CA-TRIDE compared with the conventional method is illustrated in Figure 1.

First, our TRIDE aims to address the *weak adversary* by decoupling the perturbation updates on the three components of a triplet (anchors, positive candidates, and negative candidates) into two phases. Specifically, in the anchor perturbation (ANP) phase, the anchor is perturbed, and in the candidate perturbation (CAP) phase, the positive and negative candidates are perturbed. By alternating between CAP and ANP, TRIDE leads to relatively large embedding shifts, represented by the red shadows in Figure 1, yielding a relatively stronger adversary for adversarial training. Then, our CA tackles model collapse caused by our TRIDE, using our proposed collapseness metric (denoted as \mathcal{C}) to capture the intermediate model states [27]. Specifically, \mathcal{C} prevents potential model collapse by orienting the optimization of CAP/ANP in TRIDE.

In sum, our paper makes the following three contributions:

- We propose CA-TRIDE, a novel approach to adversarial robust image retrieval based on collapse awareness (CA) and triplet decoupling (TRIDE). In particular, a new metric called collapseness is proposed to capture the intermediate model states w.r.t model collapse.
- We validate that CA-TRIDE addresses the two limitations in existing defense: *weak adversary* and *model collapse*, showing that CA-TRIDE yields noticeably larger embedding shifts, lower averaged embedding distances and lower separability, without causing model collapse.
- We identify two drawbacks of the commonly used robustness evaluation metric, ERS [33], and propose a new metric, ARS. Experimental results on three datasets show that CA-TRIDE outperforms existing methods in both ERS and ARS by 4~5%.

2. Related Work

2.1. Image Retrieval and Deep Metric Learning

Image retrieval [23] has been thriving as a surging amount of visual content has become available to the public. Deep metric learning (DML) is one of the popular methods to realize image retrieval tasks. Two main focuses of current work in DML are loss functions and data sampling methods, both of which have a crucial impact on image retrieval performance [12]. For loss functions, among other newly proposed losses, such as lifted structure loss [13], N-pair loss [18] and Multi-Similarity loss [24], triplet loss [17, 28] has been popular due to its simplicity and performance. For sampling methods, current research focuses on improving the diversity of samples within a batch to enhance the overall performance. Popular sampling strategies include random

sampling, semi-hard sampling [17], soft-hard sampling [16], distance-weighted sampling [26], etc. In this paper, we adopt the commonly used triplet loss for training DML models.

2.2. Adversarial Attacks in Deep Metric Learning

Adversarial attacks (AAs) against image retrieval primarily seek to lower the R@1 of image retrieval [9, 20, 21, 3]. These attacks, such as DAIR [2] and QAIR [8], are mostly black-box and realized through repetitive queries to get a subset of the victim model’s training set, which is subsequently used for optimizing AAs. Universal adversarial perturbations (UAPs) have also been explored for image retrieval, which works by utilizing rank-wise relationships to increase the transferability of AAs [7]. In addition, [32] explores a ranking attack that compromises the ranking results, i.e. improves or decreases the rank of certain candidates.

2.3. Adversarial Defenses in Deep Metric Learning

Current DML defenses against AAs are relatively less explored. Similar to common adversarial defense practices in image classification [30, 29, 15, 14, 34], existing defense methods in DML [33, 31] also rely on adversarial training with a triplet loss. Specifically, [33] proposed an indirect perturbation method, anti-collapse triplet (ACT), which pulls positive and negative candidates in the triplet closer to make them harder to distinguish, which consequently causes limited robustness. In their later work [31], a direct adversary called hardness manipulation (HM) [31] was proposed and achieved a better result than ACT. However, as a certain number of adversaries were found to cause the model to collapse, the authors had to resort to weak adversaries to prevent such an issue. In this paper, we specifically address the model collapse and weak adversary problems in existing defenses with our proposed CA-TRIDE.

3. Methodology

3.1. Preliminaries

Triplet Loss. Triplet loss helps the model learn an embedding space that locates semantically similar examples as closely as possible. This is achieved by minimizing $d(\mathbf{A}, \mathbf{P})$ and maximizing $d(\mathbf{A}, \mathbf{N})$ until the margin $\beta_{\mathcal{T}}$ is met. Given a triplet $\mathbb{T} = (\mathbf{A}, \mathbf{P}, \mathbf{N})$, the triplet loss $L_{\mathcal{T}}$ is defined as follows:

$$L_{\mathcal{T}}(\mathbb{T}) = d(\mathbf{A}, \mathbf{P}) - d(\mathbf{A}, \mathbf{N}) + \beta_{\mathcal{T}} \quad (1)$$

where \mathbf{A} , \mathbf{P} , and \mathbf{N} represent the anchors, positive, and negative examples, respectively. $d(\cdot, \cdot)$ calculates the average distance between two samples of the given triplet. $\beta_{\mathcal{T}}$ is the margin that defines how far the model needs to separate \mathbf{P} from \mathbf{N} , usually set within [0.2, 0.8].

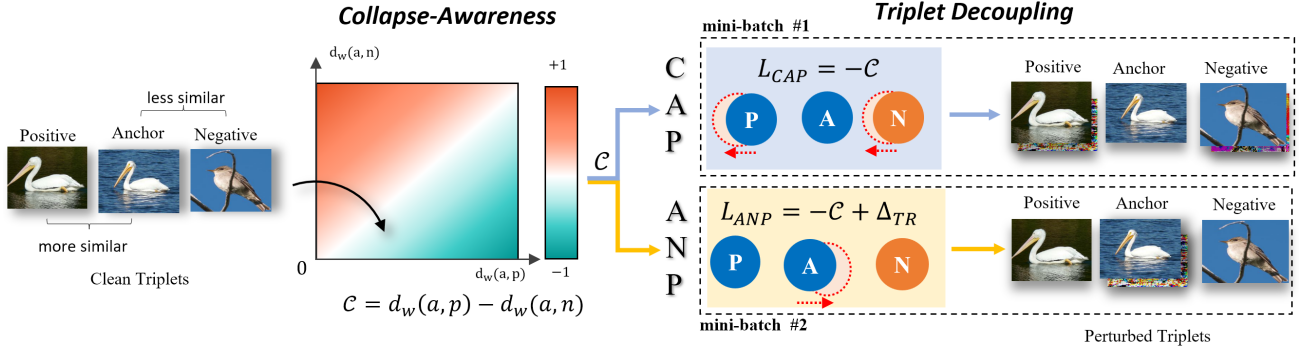


Figure 2. The working pipeline of our **CA-TRIDE** defense on a per mini-batch basis. (1) **Collapse-Awareness (CA)** first calculates the proposed collapse \mathcal{C} on the clean triplets to capture model states and then incorporates collapse into subsequent perturbation optimization. (2) **Triplet Decoupling (TRIDE)** decouples the perturbation targets on the triplets into candidate perturbation (CAP) and anchor perturbation (ANP), which are alternatively implemented across mini-batches during adversarial training, starting with CAP.

Consequently, the goal of adversarial training is otherwise: adversarially maximizing $d(\mathbf{A}, \mathbf{P})$ while minimizing $d(\mathbf{A}, \mathbf{N})$.

Hardness. Proposed in the recent work [31], the hardness of a triplet \mathbb{T} is defined as follows:

$$H(\mathbf{A}, \mathbf{P}, \mathbf{N}) = d(\mathbf{A}, \mathbf{P}) - d(\mathbf{A}, \mathbf{N}), \quad H \in [-2, 2] \quad (2)$$

Hardness determines how difficult a triplet is for a DML model to distinguish. A negative H signifies easy triplets, while a positive H denotes hard triplets. The magnitude of H determines how hard or easy the triplet is.

Adversarial Training (AT) in DML. In contrast to the standard training, the goal of AT is to learn a robust model θ on the adversarial triplet $\tilde{\mathbb{T}}$, which is acquired by adding perturbations δ into the clean triplet $\tilde{\mathbb{T}} = (\tilde{\mathbf{A}}, \tilde{\mathbf{P}}, \tilde{\mathbf{N}}) = (\mathbf{A} + \delta, \mathbf{P} + \delta, \mathbf{N} + \delta)$. Specifically, the perturbation δ is optimized by maximizing hardness H :

$$\arg \max_{\delta} H(\tilde{\mathbf{A}}, \tilde{\mathbf{P}}, \tilde{\mathbf{N}}) \quad (3)$$

where δ is bounded by a norm ϵ for imperceptibility. The specific methods for maximizing H could vary across different methods. For example, the afore-mentioned HM uses $L_{adv} = \|H_D - \tilde{H}_S\|_2^2$ to generate perturbation to increase original hardness H_S .

After the generation of perturbed triplets, these triplets are used for training an adversarially robust model Θ by optimizing:

$$\arg \min_{\theta} L_{\mathcal{T}}(\tilde{\mathbf{A}}, \tilde{\mathbf{P}}, \tilde{\mathbf{N}}; \Theta) \quad (4)$$

Our CA-TRIDE is built on AT, as shown in the per mini-batch working pipeline in Figure 2. Overall, given a mini-batch of triplets, CA first evaluates model states on clean triplets using collapse \mathcal{C} . The calculated \mathcal{C} is then

fed into the subsequent TRIDE to incorporate collapse-awareness during the optimization of perturbations to prevent model collapse by regulating the attack strength. Specifically, TRIDE starts with CAP and alternates between CAP and ANP to perturb the triplets with the dedicated adversarial losses, L_{CAP} and L_{ANP} . These perturbed triplets are then fed into the model for training, followed by another mini-batch of CA-TRIDE until the training stops. The full process of generating perturbed triplets using CA-TRIDE is described in Algorithm 1.

3.2. Collapse-Aware Adversary (CA)

To incorporate collapse-awareness in the optimization of perturbation and prevent model collapse, we first introduce *collapse* as a novel metric to capture model states proactively and accurately.

Collapse. Hard triplets (i.e. $H > 0$) are considered the main cause of model collapse due to their difficulty in optimizing, according to current research [27, 17]. Furthermore, the collapsing speed and severity depend on how many and how hard these triplets are. Although an intuitive practice is to use H as a metric, it is not a feasible option as H only “reports” model collapse *after* it occurs and cannot “forecast” it beforehand, not to mention capturing a gradual collapse. Thus, to guide subsequent counter-measurement against model collapse, we propose *Collapse* as a proactive metric for model state evaluation, denoted as \mathcal{C} :

$$\mathcal{C}(\mathbf{A}, \mathbf{P}, \mathbf{N}) = d_{\omega}(\mathbf{A}, \mathbf{P}) - d_{\omega}(\mathbf{A}, \mathbf{N}) \quad (5)$$

$d_{\omega}(\cdot, \cdot)$ is a weighting function that weighs more on near-anchor samples. $d_{\omega}(\cdot, \cdot)$ is calculated as follows:

$$d_{\omega}(\mathbf{A}, \mathbf{P}) = \frac{\sum_i^{\mathbf{A}, \mathbf{P}} (w_{p_i} \cdot d(a_i, p_i))}{\sum_i^{\mathbf{A}, \mathbf{P}} w_{p_i}} \quad (6)$$

$$w_{p_i} = \exp\left(-\lambda(d(a_i, p_i) - \min_{a_i \in \mathbf{A}, p_i \in \mathbf{P}} d(a_i, p_i))\right) \quad (7)$$

Algorithm 1 Generating Adversarial Triplets in CA-TRIDE

Require: Clean triplets $\mathbb{T} = (\mathbf{A}, \mathbf{P}, \mathbf{N})$, maximum PGD steps M , PGD step size α

Ensure: Adversarial Triplet $\tilde{\mathbb{T}}$

- 1: Initialize $\tilde{\mathbb{T}}_0 \leftarrow \mathbb{T}$
 - 2: **if** CAP **then**
 - 3: **for** $i \leftarrow 1$ to M **do**
 - 4: $\delta_i \leftarrow \alpha \nabla_{\delta} L_{CAP}(\tilde{\mathbb{T}}_{i-1})$
 - 5: $\tilde{\mathbb{T}}_i \leftarrow (\mathbf{A}, \tilde{\mathbf{P}}_{i-1} + \delta_i, \tilde{\mathbf{N}}_{i-1} + \delta_i)$
 - 6: **end for**
 - 7: **else if** ANP **then**
 - 8: **for** $i \leftarrow 1$ to M **do**
 - 9: $\delta_i \leftarrow \alpha \nabla_{\delta} L_{ANP}(\tilde{\mathbb{T}}_{i-1})$
 - 10: $\tilde{\mathbb{T}}_i \leftarrow (\tilde{\mathbf{A}}_{i-1} + \delta_i, \mathbf{P}, \mathbf{N})$
 - 11: **end for**
 - 12: **end if**
 - 13: **return** $\tilde{\mathbb{T}} \leftarrow \tilde{\mathbb{T}}_M$
-

where λ is the attention factor to determine how much attention should \mathcal{C} pay to near-anchor samples, and $\exp(\cdot)$ is conventionally adopted to map all inputs into $[0, 1]$, with a larger weight for proximity samples and a smaller value for others. $d_{\omega}(\mathbf{A}, \mathbf{N})$ can be calculated similarly. **Positive \mathcal{C} signals an impending model collapse, while negative \mathcal{C} suggests a moderate hardness for the model.**

As a cause of model collapse [27], our \mathcal{C} can detect undergoing model collapse and track the model state proactively by focusing more on proximity samples. We also evaluate both H and \mathcal{C} w.r.t tracking model states to demonstrate the superiority of \mathcal{C} , presented in Section 4.2.

Collapse-Aware Adversary. With our proposed \mathcal{C} , the adversarial goal of our subsequent perturbation optimization shifts from directing maximizing H into maximizing \mathcal{C} :

$$\arg \max_{\delta} \mathcal{C}(\tilde{\mathbf{A}}, \tilde{\mathbf{P}}, \tilde{\mathbf{N}}) \quad (8)$$

The definition of our collapse-aware adversary is intuitive as it utilizes the proposed \mathcal{C} to optimize its adversary, while \mathcal{C} also provides feedback for the optimization of the adversary to keep it aware of how well the model handles these perturbed samples. In general, the maximization goal of Eq. 8 determines the strength of AT. Since our primary goal of introducing a collapse-aware adversary is to prevent model collapse during training, we intuitively keep $\mathcal{C} \leq 0$ during the optimization of all perturbations to ensure that the adversary does not cause a severe model collapse while remaining reasonably strong enough to bring sufficient adversarial robustness.

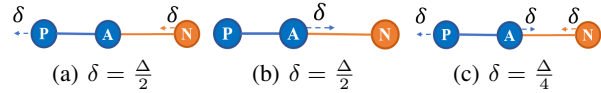


Figure 3. Illustration of the required averaged embedding shift δ to achieve the same hardness change Δ using different perturbation methods, (a) CAP, (b) ANP, and (c) conventional method. Our CAP and ANP double the averaged embedding shift in this case.

3.3. Triplet Decoupling (TRIDE)

To address the weak adversary, we propose a new AT paradigm dubbed TRIDE to essentially decouple the current perturbation method into two stages, Candidate Perturbation (CAP) and Anchor Perturbation (ANP), as shown in Figure 1. Combining with our collapse-aware adversary, Eq. 8 can be rewritten as:

$$\arg \max_{\delta} \begin{cases} \mathcal{C}(\tilde{\mathbf{A}}, \mathbf{P}, \mathbf{N}), & ANP \\ \mathcal{C}(\mathbf{A}, \tilde{\mathbf{P}}, \tilde{\mathbf{N}}), & CAP \end{cases} \quad (9)$$

As depicted in Figure 2, CAP and ANP are alternated mini-batch-wise, i.e. one perturbation method per mini-batch. We also provide a special case in Figure 3 that illustrates the difference between CAP, ANP, and the existing method, in which our TRIDE yields doubled embedding shifts.

Due to the innate difference among all perturbation methods, the resultant changes of both hardness H and collapseness \mathcal{C} also vary across methods, which also largely depends on the distribution of the triplets in the embedding space. The adversarial loss for each stage is thus designed following the innate traits of CAP and ANP, which will be introduced as follows.

Candidate Perturbation (CAP). CAP perturbs all candidates (positives and negatives) while keeping the anchors fixed during perturbation generation. L_{CAP} is intuitively designed to maximize the aforementioned collapseness \mathcal{C} in Eq. 5, by minimizing the following loss function:

$$L_{CAP} = \max(-\mathcal{C}, 0) \quad (10)$$

where the $\max(\cdot)$ term clips the loss to 0 to terminate the optimization of perturbation once $\mathcal{C} \geq 0$. In this way, the optimization of CAP becomes collapse-aware and properly stops optimization once the adversary becomes unacceptably strong for the model, preventing models from confronting severe model collapse.

CAP corrupts the global embedding (all negatives and positives) and helps the model defend against ranking attacks (i.e. disturbing the ranks of one or more samples) by enhancing **global robustness**.

Anchor Perturbation (ANP). ANP directly pushes the anchor away from the positives and towards the negatives.

Similarly to CAP, the goal of L_{ANP} is also to maximize \mathcal{C} , given below:

$$L_{ANP} = \max(-\mathcal{C} + \Delta_{TR}, 0) \quad (11)$$

ANP specializes in efficiently corrupting the local (anchor proximity) embeddings, making it a practical implementation for black-box attacks targeted at retrieval performance [2, 8], i.e. Recall attacks. To make full use of such traits and help models build better resistance against such attacks, we propose a top-rank term Δ_{TR} and a top-rank triplet L_{TR} as a top-rank pair for stronger **local** (top-rank) **robustness**.

Top-rank pair. Our proposed top-rank pair Δ_{TR} is designed to push anchors towards closest negatives further and maximize the embedding shift of anchors as \mathcal{C} approaches 0, to reinforce local corruption:

$$\Delta_{TR} = e^{\max(\mathcal{C}, 0)}(d(\mathbf{A}, \mathbf{N}_v) - d(\mathbf{A}, \mathbf{A}_0)) \quad (12)$$

where \mathbf{N}_v represents the top half of negatives, ranked by their distances to anchors, and \mathbf{A}_0 stands for original unperturbed anchors. The $exp(\cdot)$ term ensures Δ_{TR} only kicks in as \mathcal{C} approaches 0, i.e. \mathbf{A} approaches \mathbf{N} .

The top-rank triplet L_{TR} is similarly defined using the triplet loss $L_{\mathcal{J}}$, pairing with Δ_{TR} to help models capture local robustness:

$$L_{TR} = \gamma(d(\mathbf{A}, \mathbf{P}_v) - d(\mathbf{A}, \mathbf{N}_v) + \beta_{TR}) \quad (13)$$

where γ is a pre-determined coefficient, and \mathbf{P}_v is similarly defined as \mathbf{N}_v , i.e., the top half of positives ranked by their distances to the anchor.

In sum, Δ_{TR} and L_{TR} work collaboratively to further boost the local robustness of models against prevailing black-box attacks deployed on anchors (queries)[2, 8]. Δ_{TR} reinforces local corruption for stronger, targeted adversaries, and L_{TR} helps the model to capture local embeddings.

Model training. As delineated in Equation 4, perturbed triplets generated through TRIDE are subsequently used for training a robust model by optimizing:

$$\arg \min_{\Theta} \begin{cases} L_{\mathcal{J}}(\tilde{\mathbf{A}}, \mathbf{P}, \mathbf{N}; \Theta) + L_{TR}, & ANP \\ L_{\mathcal{J}}(\mathbf{A}, \tilde{\mathbf{P}}, \tilde{\mathbf{N}}; \Theta), & CAP \end{cases} \quad (14)$$

In general, our TRIDE follows the lead of \mathcal{C} to push the model to its limit by alternatively perturbing the triplets through CAP and ANP, enhancing its **global robustness** and **local robustness** respectively, without incurring disastrous model collapse. More implementation details can be found in Appendix C.

3.4. Robustness evaluation metrics

Existing metrics. Existing works use ERS as the robustness evaluation metric, including 10 attacks for evaluation (details can be found in [33]), which we categorize into ranking

attacks and recall attacks. **Ranking attacks**, such as CA+ and CA-, evaluate the robustness of the overall rankings, while **Recall attacks** focus on corrupting the proximity of anchors to lower overall retrieval performance (i.e. R@k).

However, there are fairness issues in ERS that make it infeasible for reasonable robustness evaluation: (1) *Inconsistent similarity metrics.* ERS includes TMA [20], the only cosine-similarity-based attack, as one of the attacks for robustness evaluation, which is not appropriate for evaluating models trained in the Euclidean space. Experimental results also indicate that TMA yields contradictory results against all other attacks (see Table 4 in the Appendix and Table 6 in [31]). (2) *Initial state variations.* ERSs are calculated using after-attack results, without considering the variation in the initial state before attacks. For example, in the CA+ attack (which raises the rank of a candidate over a query), despite the **randomly** selected targets, ERS ignores the variation in their before-attack ranks, e.g., 50 ± 1 . This introduces noise into ERS and makes it inaccurate. Similar issues persist for R@1 attacks. Since ERS calculates a joint total score, clean R@1 cannot become a reference for justification.

Adversarial Resistance Score. To solve the issues above, we remove TMA from evaluation metrics for fairness consideration, and ES:D is also removed as it only considers attack-caused embedding shifts and does not necessarily equal robustness. Specifically, the Adversarial Resistance Score (ARS) of an attack \mathcal{A} against a model \mathbf{M} is defined as follows:

$$\mathbb{R}_{\mathbf{M}, \mathcal{A}} = (1 - \frac{\mathcal{O}_a}{\mathcal{O}_g}) \times 100\%, \quad (15)$$

where the desired goal of the attack is \mathcal{O}_g (such as ranks or R@1) and the actual outcome of the attack is \mathcal{O}_a . Detailed calculations of ASR for different types of attacks can be found in Appendix B.

Unlike ERS, our ARS calculates the percentage of change over the attack’s intention, eliminating the variation in initial conditions for a more reasonable robustness evaluation.

4. Experiments

In this section, we conduct comprehensive experiments to demonstrate the effectiveness of our CA-TRIDE, involving its comparison to other defense baselines, the validation of CA in preventing model collapse and TRIDE in solving the weak adversary, and ablation studies on the main components of our CA-TRIDE.

4.1. Experimental settings

Models and datasets. We follow the setting of [33] and use a pre-trained ResNet-18 [4] with the last layer changed to $N=512$ as our baseline model. Evaluations are on three

Dataset	Defense	PGD	Benign Example Evaluation				Adversarial Example Evaluation (%)							Overall	Overall	
	Method	steps	R@1 ↑	R@2 ↑	mAP ↑	NMI ↑	CA+ ↑	CA- ↑	QA+ ↑	QA- ↑	ES:R ↑	LTM ↑	GTM ↑	GTT ↑	ERS ↑	ARS ↑
CUB	N/A	N/A	58.9	66.4	26.1	59.5	3.3	0.0	0.0	0.0	0.0	0.0	0.0	23.9	0.0	3.8
	ACT	32	27.5	38.2	12.2	43.0	31.0	62.9	30.2	68.5	40.3	34.2	54.2	1.0	33.9	40.3
	HM	32	34.9	45.0	19.8	47.1	31.0	62.9	33.2	69.8	51.3	47.9	78.2	2.9	36.0	47.2
	Ours	16	34.9	45.1	19.6	45.6	32.6	68.5	41.8	79.2	61.9	59.0	64.8	5.3	38.6	51.6
CARS	N/A	N/A	63.2	75.3	36.6	55.6	0.4	0.0	0.0	3.6	0.0	0.0	21.2	0.0	3.6	2.8
	ACT	32	43.4	54.6	11.8	42.9	36	68.4	35	70.2	37.6	35.3	47.7	1.6	38.6	41.4
	HM	32	60.2	71.6	33.9	51.2	38.6	74.8	39.2	75.1	50.3	61.0	76.4	8.8	46.1	52.9
	Ours	16	60.7	71.2	34.6	49.4	36	81.0	47.0	87.5	64.4	6.9	60.8	13.7	47.7	57.2
SOP	N/A	N/A	62.9	68.5	39.2	87.4	0.2	0.6	0.3	0.9	0.0	0.0	10.0	0.0	4.0	1.5
	ACT	32	47.5	52.6	25.5	84.9	48.2	90.4	45.4	91.5	44.6	45.5	58.5	15.3	50.8	54.9
	HM	32	46.8	51.7	24.5	84.7	64.0	96.8	67.4	98.0	83.5	85.0	81.0	45.6	61.6	77.7
	Ours	16	48.3	53.3	25.9	84.9	65.8	97.1	71.4	97.9	89.4	93.4	82.4	53.1	62.4	81.3

Table 1. Robustness of ACT, HM, and our CA-TRIDE under the conventional robustness metric, ERS (Empirical Robustness Score) [33], and our proposed metric, Adversarial Resistance Score (ARS).

popular datasets in image retrieval tasks, i.e. CUB-200-2011 [25], Cars-196 [6], and SOP [13]. We train our models under our CA-TRIDE framework by ADAM[5] optimizer with a 1.0×10^{-3} learning rate, a mini-batch size of 112, and training epochs of 100 under the above three datasets.

Adversaries. Adversarial perturbation is generated through PGD [11] with an optimization step $\alpha = 1/255$, 16 iterations and clipped by an l_∞ norm of $\epsilon = 8/255$. A progressive PGD step size α is also deployed to help the model balance between accuracy and robustness. All CA-TRIDE implementation details are the same unless specified. Details are given in the supplementary material.

Metrics. Benign results are given as R@1, R@2, mAP, and NMI following the setting in [31], while robustness scores are calculated using both the conventional robustness metric, ERS (Empirical Robustness Score) [33], and our proposed metric, Adversarial Resistance Score (ARS).

4.2. CA-TRIDE vs. Other Defense Methods

We compare our CA-TRIDE to the existing SOTA methods, HM [31] and ACT [33], in terms of their performance on both benign and adversarial examples, based on the above metrics. Results are presented in Table 1 (detailed results for ERS are given in Table 4 of Appendix B). We can draw the following conclusions: (1) CA-TRIDE significantly outperforms HM and ACT in almost all attacks under both ERS and ARS, which demonstrates the effectiveness of our CA-TRIDE settings. This suggests that **CA-TRIDE models can undertake stronger AT without model collapse**. (2) CA-TRIDE uses only half the PGD steps of the previous methods but exhibits higher robustness, at the cost of little or no drop in benign performances. This implies that **our TRIDE settings provide stronger adversaries and more efficient AT**.

As for the relatively lower performance of our models in TMA scores, it does not necessarily mean lower performance because all models are trained in the Euclidean space

while TMA is evaluated using cosine similarity. Moreover, it is noticeable that models with higher overall robustness (i.e. HM and ours) constantly score lower in TMA than less robust models (ACT), which contradicts all other attacks. As for GTM, this reflects the trade-off between emphasizing local robustness (top-rank samples) and global robustness (overall samples). In CA-TRIDE, we propose a top-rank pair to emphasize local robustness. However, GTM naively pushes the anchor towards the *entire* negatives rather than top-rank samples, which contradicts the goal of our top-rank pair that prioritizes top-half negatives, thus leading to relatively lower scores.

4.3. Validation of CA and TRIDE

Here we conduct comprehensive analyses to validate the individual effectiveness of our CA and TRIDE. To this end, we train the following models: an NT model trained on vanilla data, a Naive AT model trained using a conventional adversary, a CA-CAP model, a CA-ANP model, and a CA-TRIDE model (i.e. our full implementation).

CA prevents model collapse. To visualize model states, we calculate the per mini-batch average sample distances \bar{d} and use separability, defined as $\frac{d(a,n)-d(a,p)}{\bar{d}}$, to evaluate how well the model separates positive and negative samples. In particular, division by \bar{d} eliminates the influence of overall embedding changes.

As shown in the left graphs of Figure 4, benign training (black dashed line) maximizes the separation between positives and negatives, without incurring a decrease in average sample distances (i.e. \bar{d}). However, naive AT yields a drastic decrease in \bar{d} and harms separability by making it start as negative and fluctuate around 0. We thus summarise *embedding shrinkage* and *entangled samples* as two representative manifestations of model collapse. The separability of CA-CAP and CA-ANP remains positive during training, and \bar{d} undergoes a mild shrinkage. This shows the effectiveness of collapse awareness in stopping model collapse, i.e.

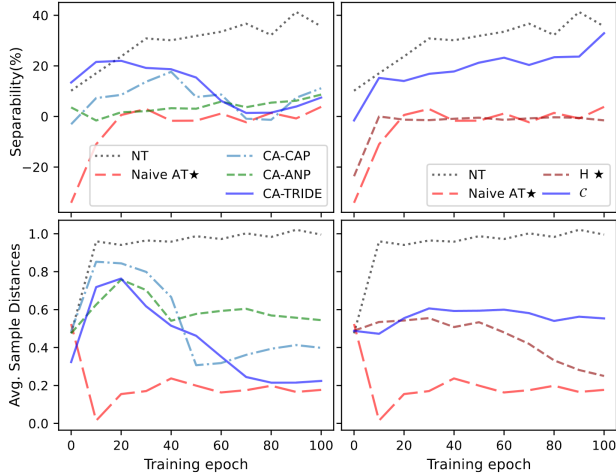


Figure 4. **Left:** Our TRIDE leads to lower separability and larger shrunk embedding distances compared with CAP/ANP, but the model remains uncollapsed thanks to the incorporation of our collapse-awareness. **Right:** Our collapseness \mathcal{C} outperforms the conventional hardness H in preventing model collapse. \star denotes model collapse, i.e. separability ≈ 0 and heavily shrunk embeddings. The dataset is CUB.

preventing embedding shrinkage and entangled samples.

Finally, to validate the superiority of \mathcal{C} as a novel metric to track model states proactively, we train two models using CA-TRIDE but with different metrics: our collapse-aware adversary and hardness-aware adversary, denoted as \mathcal{C} and H , respectively. Progressive α is disabled for a fairer comparison. Results are given in right graphs in Figure 4. The behavior of H resembles that of Naive AT, both of which confront model collapse. \mathcal{C} -oriented behaves similarly to NT, implying the superiority of our \mathcal{C} .

TRIDE solves weak adversary. To validate the effectiveness of our TRIDE, we compare the averaged embedding shifts caused by perturbations generated using three methods: HM, CAP, and ANP. All values are normalized similarly as separability to eliminate the influence of embedding shrinkage. As shown in Figure 5, our CA-CAP and CA-ANP achieve consistently larger relative embedding shifts than previous methods, especially in the later stage of the training. This demonstrates the efficacy of TRIDE in maximizing embedding shifts. Qualitative analysis also aligns with this result, as given in Appendix A. To further investigate the individual effectiveness of TRIDE, we train three model variants without using CA, i.e. a naive CAP model, a naive ANP model, and a naive TRIDE model. Their R@1 results are 4.4%, 7.8% and 0.8%, respectively, indicating that, as expected, both CAP/ANP/TRIDE could yield strong enough adversaries that could cause model collapse.

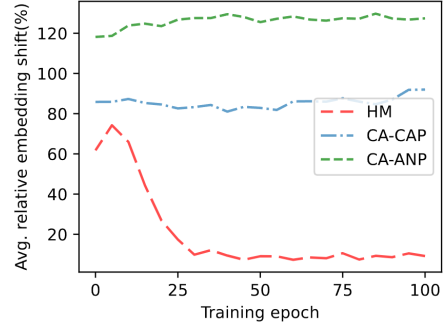


Figure 5. Our CA-ANP and CA-CAP cause substantially larger embedding shifts than HM. The dataset is CUB.

4.4. Ablation Studies

TRIDE vs. CAP/ANP. As shown in Table 2, deploying TRIDE does not necessarily reduce the overall strength of AT. Contrarily, CA-CAP and CA-ANP models emphasize differently on robustness. CA-CAP exhibits better robustness in almost all ranking attacks than CA-ANP, while the latter is more robust against Recall attacks, which echoes our intention of designing CAP and ANP. More importantly, combining CAP and ANP provides well-rounded robustness across all attacks and achieves the best overall robustness in both ARS and ERS.

Top-rank pair. As discussed in Section 3.3, the top-rank pair is incorporated to reinforce local corruption in ANP and help the model capture top-rank robustness against R@k attacks. According to the results presented in Table 3, the model with Δ_{TR} only already gains over 10% of robustness boost against all attacks compared to its counterpart without our top-rank pair, with an impressive enhancement of performance on clean examples. This indicates the novelty of Δ_{TR} regarding the AT efficiency. Furthermore, when paired with the top-rank triplet L_{TR} , our model further acquires a noticeable increase in robustness against all Recal attacks. On the other hand, the marginal drop w.r.t. ranking attacks (i.e. CA+, CA-, and QA+) suggests that emphasis on local robustness may trade off global robustness. We would explore how to achieve an optimal trade-off in future work.

Hyperparameters. We also investigate how our models behave under different hyperparameters, i.e. the attention factors λ in \mathcal{C} and the triplet loss margin β_{TR} in L_{TR} . For λ , as introduced in Eq. 5, it determines how much attention should \mathcal{C} pay to near-anchor samples. As λ increases, \mathcal{C} would focus more on samples that are closer to anchors and pay less attention to those farther samples. Note that when $\lambda = 0$, our collapseness falls back to hardness as it treats all examples identically. Results are presented in Figure 6. Overall, our CA-TRIDE is insensitive to λ , while a too large λ could further increase the clean accuracy but harm the robustness. Hence, we choose the value of λ that yields the closest R@1 performance as HM for a fair comparison, i.e.

Defense Method	R@1↑	Adversarial Example Evaluation (ARS) (%)								Overall ERS↑	Overall ARS↑
		CA+↑	CA-↑	QA+↑	QA-↑	ES:R ↑	LTM↑	GTM ↑	GTT ↑		
CA-ANP	34.2	27.4	56.7	35.6	73.3	57.3	61.1	65.8	5.1	34.0	47.8
CA-CAP	33.8	34.2	68.0	52.2	70.8	51.2	47.6	60.7	3.1	37.9	48.5
CA-TRIDE	34.9	32.6	68.5	41.8	79.2	61.9	59.0	64.8	5.3	38.6	51.6

Table 2. Ablation study on CA-TRIDE vs. CA-CAP/-ANP. The dataset is CUB.

Defense Method	R@1↑	Adversarial Example Evaluation (ARS) (%)								Overall ERS↑	Overall ARS↑
		CA+↑	CA-↑	QA+↑	QA-↑	ES:R ↑	LTM↑	GTM ↑	GTT ↑		
w/o TPR	32.7	27.8	60.2	36.6	69.1	46.2	26.3	47.4	0.7	33.26	39.3
w/o L_{TR}	34.6	34.6	70.0	43.4	79.1	57.8	54.9	60.7	4.0	38.4	50.6
CA-TRIDE	34.9	32.6	68.5	41.8	79.2	61.9	59.0	64.8	5.3	38.6	51.6

Table 3. Ablation study on the top-rank pair (TRP), i.e. $\Delta_{TR+L_{TR}}$. The dataset is CUB.

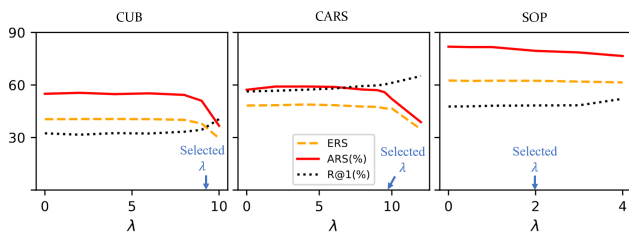


Figure 6. Ablation study on the attention factor λ .

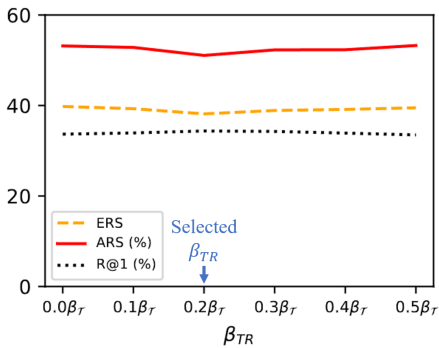


Figure 7. Ablation study on the triplet loss margin β_{TR} in L_{TR} . The dataset is CUB.

10 for CUB, 9.5 for CARS, and 2 for SOP.

For β_{TR} in L_{TR} , it functions similarly to the $\beta_{\mathcal{J}}$ in the triplet loss- determining how hard should the model keep positives and negatives separated, or more precisely, top-rank positives and negatives. Likewise, L_{TR} is essentially a variant triplet loss calculated using only top-rank examples from all examples, and we thus evaluate the β_{TR} as a proportion of $\beta_{\mathcal{J}}$, ranging from 0 to 50%. As shown in Figure 7, no significant changes in robustness can be found as β_{TR} varies. Therefore, similar to λ , we choose the value of β_{TR} that yields the closest R@1 performance as HM for

a fair comparison, i.e. $\beta_{TR} = 0.2\beta_{\mathcal{J}}$.

5. Conclusion

In this paper, we have proposed CA-TRIDE, a novel approach to training adversarially robust image retrieval models. CA-TRIDE addresses two well-recognized limitations: weak adversary and model collapse. Specifically, TRIDE yields a strong adversary by spatially decoupling the perturbation targets into the anchor and the two candidates within a triplet. To offset the model collapse enhanced by the strong adversary in TRIDE, CA further captures intermediate model states based on a novel concept, collapsesness, and incorporates it into the subsequent optimization of perturbations. In addition, we also examine the commonly used robustness evaluation metric, ERS, and identify its two drawbacks. Therefore, we propose a new metric called ARS. Extensive experiments on three datasets validate the priority of our CA-TRIDE in both ERS and ARS.

6. Impact Statement

This paper presents work that aims to advance the field of adversarial defense in image retrieval. Potential societal consequences of our work are less influential and have become scientific consensus, none of which we feel must be specifically highlighted here.

References

- [1] Jiawang Bai, Bin Chen, Yiming Li, Dongxian Wu, Weiwei Guo, Shu-Tao Xia, and En-Hui Yang. Targeted attack for deep hashing based retrieval. *CoRR*, abs/2004.07955, 2020.
- [2] Mingyang Chen, Junda Lu, Yi Wang, Jianbin Qin, and

- Wei Wang. Dair: A query-efficient decision-based attack on image retrieval systems. In *Proceedings of the 44th International ACM SIGIR Conference on Research and Development in Information Retrieval*, SIGIR '21, page 1064–1073, New York, NY, USA, 2021. Association for Computing Machinery.
- [3] Yan Feng, Bin Chen, Tao Dai, and Shutao Xia. Adversarial attack on deep product quantization network for image retrieval. *CoRR*, abs/2002.11374, 2020.
- [4] Kaiming He, Xiangyu Zhang, Shaoqing Ren, and Jian Sun. Deep residual learning for image recognition. *CoRR*, abs/1512.03385, 2015.
- [5] Diederik P Kingma and Jimmy Ba. Adam: A method for stochastic optimization. *arXiv preprint arXiv:1412.6980*, 2014.
- [6] Jonathan Krause, Michael Stark, Jia Deng, and Li Fei-Fei. 3d object representations for fine-grained categorization. In *Proceedings of the IEEE international conference on computer vision workshops*, pages 554–561, 2013.
- [7] Jie Li, Rongrong Ji, Hong Liu, Xiaopeng Hong, Yue Gao, and Qi Tian. Universal perturbation attack against image retrieval. In *2019 IEEE/CVF International Conference on Computer Vision (ICCV)*, pages 4898–4907, 2019.
- [8] Xiaodan Li, Jinfeng Li, Yuefeng Chen, Shaokai Ye, Yuan He, Shuhui Wang, Hang Su, and Hui Xue. QAIR: practical query-efficient black-box attacks for image retrieval. *CoRR*, abs/2103.02927, 2021.
- [9] Zhuoran Liu, Zhengyu Zhao, and Martha A. Larson. Who’s afraid of adversarial queries? the impact of image modifications on content-based image retrieval. *CoRR*, abs/1901.10332, 2019.
- [10] Junda Lu, Mingyang Chen, Yifang Sun, Wei Wang, Yi Wang, and Xiaochun Yang. A smart adversarial attack on deep hashing based image retrieval. In *Proceedings of the 2021 International Conference on Multimedia Retrieval*, ICMR '21, page 227–235, New York, NY, USA, 2021. Association for Computing Machinery.
- [11] Aleksander Madry, Aleksandar Makelov, Ludwig Schmidt, Dimitris Tsipras, and Adrian Vladu. Towards deep learning models resistant to adversarial attacks. *arXiv preprint arXiv:1706.06083*, 2017.
- [12] Kevin Musgrave, Serge Belongie, and Ser-Nam Lim. A metric learning reality check. In *Computer Vision—ECCV 2020: 16th European Conference, Glasgow, UK, August 23–28, 2020, Proceedings, Part XXV 16*, pages 681–699. Springer, 2020.
- [13] Hyun Oh Song, Yu Xiang, Stefanie Jegelka, and Silvio Savarese. Deep metric learning via lifted structured feature embedding. In *Proceedings of the IEEE conference on computer vision and pattern recognition*, pages 4004–4012, 2016.
- [14] Tianyu Pang, Xiao Yang, Yinpeng Dong, Kun Xu, Jun Zhu, and Hang Su. Boosting adversarial training with hypersphere embedding. *Advances in Neural Information Processing Systems*, 33:7779–7792, 2020.
- [15] Marine Picot, Francisco Messina, Malik Boudiaf, Fabrice Labeau, Ismail Ben Ayed, and Pablo Piantanida. Adversarial robustness via fisher-rao regularization. *IEEE Transactions on Pattern Analysis and Machine Intelligence*, pages 1–1, 2022.
- [16] Karsten Roth, Timo Milbich, Samarth Sinha, Praateek Gupta, Bjorn Ommer, and Joseph Paul Cohen. Revisiting training strategies and generalization performance in deep metric learning. In *International Conference on Machine Learning*, pages 8242–8252. PMLR, 2020.
- [17] Florian Schroff, Dmitry Kalenichenko, and James Philbin. Facenet: A unified embedding for face recognition and clustering. *CoRR*, abs/1503.03832, 2015.
- [18] Kihyuk Sohn. Improved deep metric learning with multi-class n-pair loss objective. *Advances in neural information processing systems*, 29, 2016.
- [19] Christian Szegedy, Wojciech Zaremba, Ilya Sutskever, Joan Bruna, Dumitru Erhan, Ian Goodfellow, and Rob Fergus. Intriguing properties of neural networks. *arXiv preprint arXiv:1312.6199*, 2013.
- [20] Giorgos Tolias, Filip Radenovic, and Ondrej Chum. Targeted mismatch adversarial attack: Query with a flower to retrieve the tower. *CoRR*, abs/1908.09163, 2019.
- [21] Hongjun Wang, Guangrun Wang, Ya Li, Dongyu Zhang, and Liang Lin. Transferable, controllable, and inconspicuous adversarial attacks on person re-identification with deep mis-ranking. *CoRR*, abs/2004.04199, 2020.
- [22] Jian Wang, Feng Zhou, Shilei Wen, Xiao Liu, and Yuanqing Lin. Deep metric learning with angular loss. In *Proceedings of the IEEE International Conference on Computer Vision (ICCV)*, Oct 2017.
- [23] Jiang Wang, Yang Song, Thomas Leung, Chuck Rosenberg, Jingbin Wang, James Philbin, Bo Chen, and Ying Wu. Learning fine-grained image similarity with deep ranking. In *Proceedings of the IEEE conference on computer vision and pattern recognition*, pages 1386–1393, 2014.

-
- [24] Xun Wang, Xintong Han, Weilin Huang, Dengke Dong, and Matthew R Scott. Multi-similarity loss with general pair weighting for deep metric learning. In *Proceedings of the IEEE/CVF conference on computer vision and pattern recognition*, pages 5022–5030, 2019.
- [25] Peter Welinder, Steve Branson, Takeshi Mita, Catherine Wah, Florian Schroff, Serge Belongie, and Pietro Perona. Caltech-ucsd birds 200. Technical Report CNS-TR-201, Caltech, 2010.
- [26] Chao-Yuan Wu, R Manmatha, Alexander J Smola, and Philipp Krahenbuhl. Sampling matters in deep embedding learning. In *Proceedings of the IEEE international conference on computer vision*, pages 2840–2848, 2017.
- [27] Hong Xuan, Abby Stylianou, Xiaotong Liu, and Robert Pless. Hard negative examples are hard, but useful. In Andrea Vedaldi, Horst Bischof, Thomas Brox, and Jan-Michael Frahm, editors, *Computer Vision – ECCV 2020*, pages 126–142, Cham, 2020. Springer International Publishing.
- [28] Baosheng Yu, Tongliang Liu, Mingming Gong, Changxing Ding, and Dacheng Tao. Correcting the triplet selection bias for triplet loss. In *Proceedings of the European Conference on Computer Vision (ECCV)*, pages 71–87, 2018.
- [29] Hongyang Zhang, Yaodong Yu, Jiantao Jiao, Eric Xing, Laurent El Ghaoui, and Michael Jordan. Theoretically principled trade-off between robustness and accuracy. In *International conference on machine learning*, pages 7472–7482. PMLR, 2019.
- [30] Yaoyao Zhong and Weihong Deng. Adversarial learning with margin-based triplet embedding regularization. In *Proceedings of the IEEE/CVF international conference on computer vision*, pages 6549–6558, 2019.
- [31] Mo Zhou and Vishal M Patel. Enhancing adversarial robustness for deep metric learning. In *Proceedings of the IEEE/CVF Conference on Computer Vision and Pattern Recognition*, pages 15325–15334, 2022.
- [32] Mo Zhou, Le Wang, Zhenxing Niu, Qilin Zhang, Yinghui Xu, Nanning Zheng, and Gang Hua. Practical relative order attack in deep ranking. *CoRR*, abs/2103.05248, 2021.
- [33] Mo Zhou, Le Wang, Zhenxing Niu, Qilin Zhang, Nanning Zheng, and Gang Hua. Adversarial attack and defense in deep ranking. *CoRR*, abs/2106.03614, 2021.
- [34] Jianing Zhu, Jingfeng Zhang, Bo Han, Tongliang Liu, Gang Niu, Hongxia Yang, Mohan S. Kankanhalli, and Masashi Sugiyama. Understanding the interaction of adversarial training with noisy labels. *CoRR*, abs/2102.03482, 2021.

A. Theoretical Analysis of weak adversary

In this section, we provide a qualitative analysis of how and why the weak adversary leads to minimized embedding shifts, which necessitates our triplet decoupling (TRIDE) mechanism.

As discussed in the main text of the paper, the current adversarial perturbation δ is acquired by:

$$\arg \max_{\delta} H(\tilde{\mathbf{A}}, \tilde{\mathbf{P}}, \tilde{\mathbf{N}}) \quad (16)$$

Essentially, although the specific adversarial losses L_{adv} vary across methods, the general goal of L_{adv} is to adversarially maximize H . Thus, we denote the consequential change caused by the perturbation as Δ_H , defined as follows:

$$\Delta_H = H(\tilde{\mathbf{A}}, \tilde{\mathbf{P}}, \tilde{\mathbf{N}}) - H(\mathbf{A}, \mathbf{P}, \mathbf{N}) \quad (17)$$

As mentioned in the main paper, unlike AT in image classification, AT in DML has multiple choices for perturbation targets (anchors \mathbf{A} , positives \mathbf{P} , and negatives \mathbf{N}). The average embedding shift of the perturbed targets depends on two factors: the angle between \bar{a}_n and \bar{a}_p , denoted as θ [22], and the perturbation methods, denoted as \mathcal{P} . We will then determine how these factors influence the overall embedding shifts.

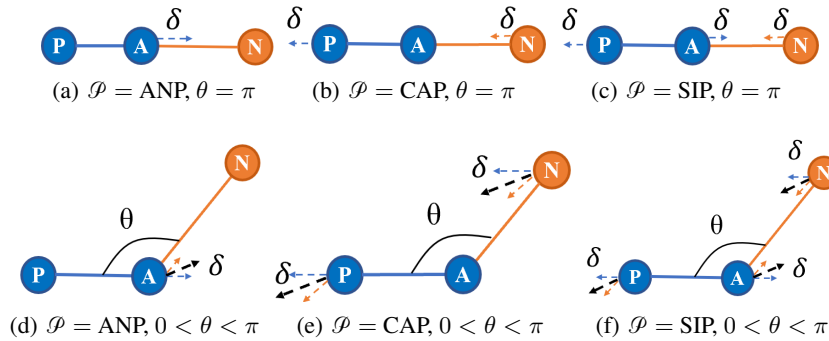


Figure 8. Demonstration on scenarios of different angle θ and perturbation method. Δ denotes the average embedding shifts of perturbed samples. ANP for anchor perturbation (only perturbs anchors), CAP for candidates perturbation (only perturbs candidates), and SIP for simultaneous perturbation (perturbs all the triplets). $\pi < \theta < 2\pi$ is omitted due to symmetry.

As shown in Figure 8, θ influences **how the perturbation changes the overall hardness**. In other words, with the same embedding shifts, θ determines the proportion of embedding shifts that transfer to Δ_H . To calculate this proportion, we calculate a function γ_θ of θ . Hence, given $\gamma(\theta)$ and a embedding shift δ , Δ_H is given by:

$$\Delta_H = \gamma_\theta \cdot \delta \quad (18)$$

According to Figure 8, γ_θ could range from 0 ($\theta = 0$, *i.e.*, $\Delta_H = 0$) to 2 ($\theta = \pi$, *i.e.*, $\Delta_H = 2\delta$).

A.1. Perturbation targets

Perturbation methods \mathcal{P} determine the total number of selected targets, (*i.e.*, 1, 2 or 3), influencing how the desired embedding shift Δ_H is allocated to all perturbation targets. A general way to understand the idea is like assigning a certain amount of tasks (target hardness). The more people (samples) get assigned, the fewer tasks (embedding shifts) each person would have.

For analysis, we assume that all perturbed targets move identically by Δ . In other words, $d_{a,\tilde{a}} = \delta_{ANP}$ for anchor perturbation (ANP), and $d_{p,\tilde{p}} = d_{n,\tilde{n}} = \delta_{CAP}$ for candidate perturbation (CAP), and $d_{a,\tilde{a}} = d_{p,\tilde{p}} = d_{n,\tilde{n}} = \delta_{SIP}$ for simultaneous perturbation (SIP), namely the existing method.

A.2. Calculations

To calculate the averaged embedding shifts given θ and \mathcal{P} , we need to determine how much of each perturbed sample needs to move to achieve the required hardness increase $\Delta_H - H(\mathbb{T})$. We further drop the term $H(\mathbb{T})$ as it is identical for the

same initial triplet. **Note that to simplify the calculation, we assume all perturbed samples have identical embedding shifts.** We can now qualitatively demonstrate how different perturbation methods \mathcal{P} and θ determine the averaged overall embedding shifts δ given the same Δ_H , in a special-to-general manner:

(1) *Special case:* $\theta = \pi$. For $\mathcal{P} = \text{ANP}$, as shown in Figure 8(a), the gradient to increase $d(a, p)$ aligns with the gradient to decrease $d(a, n)$, which doubles the hardness shift caused by δ_{ANP} . Thus, we can obtain the average embedding shift δ_{ANP} of ANP follows:

$$\begin{aligned}\gamma_\theta \cdot d_{a,\bar{a}} &= \Delta_H \\ 2\delta_{\text{ANP}} &= \Delta_H \\ \delta_{\text{ANP}} &= \frac{\Delta_H}{2}\end{aligned}\tag{19}$$

Turning to $\mathcal{P} = \text{CAP}$, as demonstrated in Figure 8(b), $\gamma_\theta = 1$, and δ_{CAP} given as follows:

$$\begin{aligned}\gamma_\theta \cdot d_{p,\bar{p}} + \gamma_\theta \cdot d_{n,\bar{n}} &= \Delta_H \\ \delta_{\text{CAP}} + \delta_{\text{CAP}} &= \Delta_H \\ \delta_{\text{CAP}} &= \frac{\Delta_H}{2}\end{aligned}\tag{20}$$

For their combination, SIP leads to the least average embedding shift (as shown in Figure 8(c)), which can be similarly calculated :

$$\begin{aligned}\gamma_\theta \cdot d_{a,\bar{a}} + \gamma_\theta \cdot d_{p,\bar{p}} + \gamma_\theta \cdot d_{n,\bar{n}} &= \Delta_H \\ 2\delta_{\text{SIP}} + \delta_{\text{SIP}} + \delta_{\text{SIP}} &= \Delta_H \\ \delta_{\text{SIP}} &= \frac{\Delta_H}{4}\end{aligned}\tag{21}$$

In this case, by comparing Eq. 19, Eq. 20, and Eq. 21, the overall average embedding shift of ANP and CAP is twice the average embedding shift of SIP.

(2) *General cases:* $0 < \theta < \pi$. For ANP, as shown in Figure 8(d), γ_θ becomes a function of θ . Through geometric calculation, we obtain the approximation of γ_θ , given as follows:

$$\gamma_\theta = 2\cos\left(\frac{\pi - \theta}{2}\right)\tag{22}$$

Then, δ_{ANP} of ANP is calculated as:

$$\begin{aligned}\gamma_\theta \cdot d_{a,\bar{a}} &= \Delta_H \\ 2\cos\left(\frac{\pi - \theta}{2}\right) \cdot \delta_{\text{ANP}} &= \Delta_H \\ \delta_{\text{ANP}} &= \frac{\Delta_H}{2\cos\left(\frac{\pi - \theta}{2}\right)}\end{aligned}\tag{23}$$

This result can be verified by simply inserting $\theta = \pi$ into Eq. 23, which gives the same result in Eq. 19.

Similar to ANP, CAP can be regarded as applying an equivalent perturbation to \mathbf{P} and \mathbf{N} , with γ_θ becoming half of ANP, (*i.e.*, half of $2\cos\left(\frac{\pi - \theta}{2}\right)$):

$$\begin{aligned}\gamma_\theta \cdot d_{p,\bar{p}} + \gamma_\theta \cdot d_{n,\bar{n}} &= \Delta_H \\ 2 \times \cos\left(\frac{\pi - \theta}{2}\right) \cdot \delta_{\text{CAP}} &= \Delta_H \\ \delta_{\text{CAP}} &= \frac{\Delta_H}{2\cos\left(\frac{\pi - \theta}{2}\right)}\end{aligned}\tag{24}$$

For SIP, δ_{SIP} can once again be calculated by combining CAP and ANP:

$$\begin{aligned}\gamma_\theta \cdot d_{a,\bar{a}} + \gamma_\theta \cdot d_{p,\bar{p}} + \gamma_\theta \cdot d_{n,\bar{n}} &= \Delta_H \\ 4\cos\left(\frac{\pi - \theta}{2}\right)\delta_{SIP} &= \Delta_H \\ \delta_{SIP} &= \frac{\Delta_H}{4\cos\left(\frac{\pi - \theta}{2}\right)}\end{aligned}\quad (25)$$

Finally, we can compare SIP with CAP + ANP in more general cases ($0 < \theta < \pi$) by comparing Eq. 23, Eq. 24 and Eq. 25. Ideally, with the exactly identical θ , $\Delta_{CAP,ANP}$ is still two times of δ_{SIP} . However, in practical scenarios, there will be a phase difference most of the time. Hence, the magnitude ratio of CAP + ANP over SIP in more general cases can be given as follows:

$$\frac{\Delta_{CAP,ANP}}{\delta_{SIP}} = \frac{2\cos\left(\frac{\pi - \theta_1}{2}\right)}{\cos\left(\frac{\pi - \theta_2}{2}\right)}\quad (26)$$

For $0 < \theta < \pi$, the denominator of the ratio can be regarded as a coefficient ranging from 0 to 1, with most of the time less than 1. This implies that this denominator mostly acts as an amplifier, making the overall ratio even larger. Due to symmetry, the scenario when $\pi < \theta < 2\pi$ is identical to what has been discussed. In other words, despite some variation, Eq. 26 aligns with the experimental results shown in Figure 5, which suggests that **our CAP + ANP setting outperforms the extant SIP in terms of maximizing the average embedding shift under the same perturbation.**

A.3. Conclusions

Our analysis is also validated experimentally in Section 4.2. Our Tride consistently outperforms SIP w.r.t. the average embedding shift under perturbation, with the largest gap being almost 4 times the averaged embedding shifts of existing methods (SIP).

Our theoretical analysis and experimental results demonstrate that the existing method leads to a significantly decreased perturbation-caused embedding shift compared to our TRIDE (CAP+ANP) setting. Consequently, the perturbation generated likewise is much weaker than the perturbation optimized using TRIDE.

Another reason for TRIDE is that simultaneous perturbation is not a practical method considering many existing attacks against DML. In black-box scenarios, most existing attacks are achieved by ANP[8, 2, 32, 7], which is more practical and effective.

B. Detailed Calculations of Adversarial Resistance Scores

Ranking Attacks. For attacks targeted at ranking, given an attack \mathcal{A} , we first calculate the goal of the attack \mathcal{O}_g . Taking CA+ as an example, given a query q , CA+ aims to increase the rank of a random candidate for the query q . For a random candidate i , we assume that it has an initial rank r for q , denoted as r_{qi} , and its rank becomes \tilde{r}_{qi} after CA+ attack. Note that the goal of CA+ is to increase r_{qi} to the highest rank, *i.e.*, $r = 0$. In other words, for this trial of CA+ attack, $\mathcal{O}_g = r_{qi}$ and $\mathcal{O}_a = |r_{qi} - \tilde{r}_{qi}|$. Hence, $\mathbb{R}_{M,CA+}$ can be calculated as follows:

$$\begin{aligned}\mathbb{R}_{M,CA+} &= \left(1 - \frac{\mathcal{O}_a}{\mathcal{O}_g}\right) \times 100\% \\ &= \left(1 - \frac{|r_{qi} - \tilde{r}_{qi}|}{r_{qi}}\right) \times 100\%\end{aligned}\quad (27)$$

$$(28)$$

Similarly, AR all rank attacks (CA+, CA-, QA+, QA-) can be calculated likewise:

$$\mathbb{R}_{M,(CA+,CA-,QA+,QA-)} = \left(1 - \frac{|r_{qi} - \tilde{r}_{qi}|}{r_{qi}}\right) \times 100\% \quad (29)$$

Dataset	Defense	PGD Method	Benign Example Evaluation					Adversarial Example Evaluation (ERS)									ERS↑
			steps	R@1↑	R@2↑	mAP↑	NMI↑	CA+↑	CA-↓	QA+↑	QA-↓	TMA↓	ES:D↓	ES:R↑	LTM↑	GTM↑	
CUB	N/A	N/A	58.9	66.4	26.1	59.5	0.0	100	0.0	99.9	0.883	1.76	0.0	0.0	14.1	0.0	3.3
	ACT	32	27.5	38.2	12.2	43.0	15.5	37.7	15.1	32.2	0.47	0.82	11.1	9.4	14.9	1.0	33.9
	HM	32	34.9	45.0	19.8	47.1	15.5	37.7	16.6	30.9	0.75	0.50	17.9	16.7	27.3	2.9	36.0
	Ours	16	34.9	45.1	19.6	45.6	16.7	31.1	20.9	21.1	0.968	0.163	21.6	20.6	22.6	5.1	38.6
CARS	N/A	N/A	63.2	75.3	36.6	55.6	0.2	100	0.1	97.3	0.874	1.816	0.0	0.0	13.4	0.0	3.6
	ACT	32	43.4	54.6	11.8	42.9	18.0	32.3	17.5	30.5	0.38	0.76	16.3	15.3	20.7	1.6	38.6
	HM	32	60.2	71.6	33.9	51.2	19.3	25.9	19.6	25.7	0.65	0.45	30.3	36.7	46	8.8	46.1
	Ours	16	60.7	71.2	34.6	49.4	17.7	20.3	23.5	12.9	0.964	0.131	39.1	40.6	36.9	13.7	47.7
SOP	N/A	N/A	62.9	68.5	39.2	87.4	0.1	99.3	0.2	99.1	0.845	1.685	0.0	0.0	6.3	0.0	4.0
	ACT	32	47.5	52.6	25.5	84.9	24.1	10.5	22.7	9.4	0.25	0.53	21.2	21.6	27.8	15.3	50.8
	HM	32	46.8	51.7	24.5	84.7	32	4.2	33.7	3.0	0.61	0.20	39.1	39.8	37.9	45.6	61.6
	Ours	16	48.3	53.3	25.9	84.9	32.3	3.7	36.0	2.6	0.804	0.14	43.2	45.1	39.8	53.1	62.4

Table 4. Robustness of ACT, HM, and our CA-TRIDE under the current metric, Empirical Robustness Score (ERS).

Recall Attacks. The evaluation of R@k attacks is much simpler as these attacks seek to lower the R@1. Thus, given a model M with initial R@1 μ_M and its after-attack R@1 $\tilde{\mu}_M$, all R@k attacks’ intention is to lower μ_M to 0, i.e., $\mathcal{O}_g = \mu_M$, $\mathcal{O}_a = \tilde{\mu}_M$. Hence, $\mathbb{R}_{M,(ES,LTM,GTM)}$ can be calculated as follows:

$$\begin{aligned} \mathbb{R}_{M,(ES,LTM,GTM)} &= \left(1 - \frac{\mu_M - \tilde{\mu}_M}{\mu_M}\right) \times 100\% \\ &= \frac{\tilde{\mu}_M}{\mu_M} \times 100\% \end{aligned} \quad (30)$$

In essence, our proposed ARS quantifies the robustness of a model based on how well the attack achieves its goal on this model. Initial state variation is eliminated by calculating the difference instead of evaluating pure results.

C. Implementation details

Parameters. For the top-rank triplet L_{TR} , $\gamma = 0.5$ and the triplet margin in L_{TR} is $\beta_{TR} = 0.04$.

Hardness adjustment. To help the model balance between learning meaningful information and acquiring robustness, we apply a simple epoch-wise adjustment strategy to mini-batch sampling and perturbation adding.

For mini-batch sampling, we follow the semi-hard sampling [17], which samples hard examples within a given range $d(a, p) < d(a, n) < d(a, p) + \eta$, and apply an epoch-wise strategy to η :

$$\eta = \eta_0 \left(1 - \left(\frac{n}{2 \times n_{total}}\right)^2\right) \quad (31)$$

where η_0 is the preset margin of semi-hard sampling, n stands for the current number of epoch, and n_{total} stands for the total number of epochs.

For perturbation adding, we similarly multiply the PGD step size α by $\frac{n}{n_{total}}$ to enable a gradually increasing adversary strength.